# Molecular Solvation in Phosphonium Ionic Liquids

A Senior Honors Thesis

Presented in Partial Fulfillment of the Requirements
For graduation in the College Honors Program

By
Kathleen M. Barra
Chemistry Major

The College at Brockport
May 2011

Thesis Director: Dr. Mark P. Heitz, Associate Professor, Chemistry

This paper was submitted on May 10, 2011 to the Thesis Committee of the Department of Chemistry and to the Director of the Honors Program at the State University of New York, College at Brockport, in completion of the thesis requirement specified in the guidelines for the award of Honors in Chemistry.

We the undersigned have read this thesis and recommend the award of Honors in Chemistry to Kathleen M. Barra upon completion of all requirements for graduation.

_____ _____

Mark P. Heitz, Ph. D. Date
Research Mentor

_____ _____

Michael A. Brown, Ph. D. Date
For the Thesis Committee

_____ _____

Markus M. Hoffmann, Ph. D. Date
For the Thesis Committee

The Faculty of the Department of Chemistry, acting upon the recommendation of the Thesis Committee, recommends that Kathleen M. Barra be granted Honors in Chemistry.

_____ _____

Stephen A. Godleski, Ph. D. Date
Chair, Department of Chemistry

**Acknowledgements**

This project would not have been possible without the assistance of a number of individuals and organizations. I would like to thank the Chemistry Department at the College at Brockport for all their support and guidance. Their love for chemistry and encouragement to always try my best while learning from my mistakes has been inspiring. I would like to thank the Brockport Summer Research Foundation which provided funding for eight weeks of summer research. Without this funding I would not have been able to have this amazing opportunity. I would also like to personally thank my research mentor, Dr. Mark Heitz. Without his constant reviewing and motivation this thesis would never be done. He has taught me a great deal of laboratory and presentation skills that will help me in all aspects of my future.

I would also like to thank my family and friends. My family has been a constant support system throughout the years and has always encouraged me to do my best. My friends have been my family away from home and without them I would have been lost in finishing this thesis.

## Table of Contents

## List of Figures

Page

## List of Tables

Page

## Abstract

The goal of this research is to understand the solvation dynamics of coumarin 153 (C153) in an environmentally-friendly room temperature phosphonium ionic liquid (RTPIL) solvent. With virtually no vapor pressure, ILs are attracting attention as potential “green” replacements for conventional volatile organic solvents. ILs are also known for chemical stability, non-flammability and recycling potential. C153 is a prototypical fluorescent molecule known for its spectral sensitivity when in solution making it ideal for these studies. Neat trihexyltetradecyl phosphonium chloride (PIL-Cl) and methanol (MeOH) solvents were used to form an array of PIL-Cl mixtures spanning the complete range of mol fraction, in which C153 was dissolved. Solvation of C153 was determined using steady-state and time-resolved fluorescence spectroscopy. The C153 steady-state data shows a systematic blue shift as PIL-Cl is added to solution. The system is at net higher energy at high mol fraction PIL-Cl implying that C153/PIL-Cl interactions are less favorable compared to C153/MeOH. The solute emission intensity is quenched most effectively at a mol fraction of ~0.03 PIL-Cl suggesting that the solvent-solute interactions are most unique in this range of mol fraction. Similarly, the lifetime data show a minimum value at ~0.03 mol fraction PIL-Cl, also implying quenching of the probe at this relative solution composition. C153 is better solvated, more relaxed, at MeOH-rich mol fractions. Solvation dynamics are characterized by time-resolved Stokes shift measurements. The time-resolved center of gravity and associated solvation correlation function, *C(t)*, show that solvation of C153 occurs at a faster rate in solutions of lower mol fraction PIL-Cl. The solvation times correlate to solvent viscosity. PILs showed slower solvation due to much larger viscosities than MeOH.

# Chapter 1

# Introduction

## 1.1 Ionic Liquids

Ionic liquids (ILs) are salts that exist in the liquid state at room temperature (~25 $^{o}$C). Room temperature ionic liquids (RTILs) are of particular interest as novel solvents since salts usually have very high melting points (~1000 $^{o}$C) and are solids at room temperature, e.g. sodium chloride or table salt. In addition, RTILs have recently attracted attention as "green" substitutes for conventional organic solvents in many applications because of their desirable physical properties.[1,2,3] RTILs have a negligible vapor pressure so they do not contribute emissions into the atmosphere.[4,5,6,7] Other properties of these green solvents are chemical stability, nonflammability, and ease of recycling.[8,9] Some RTILs are stable to temperatures greater than 300$^{o}$C.[10] Examples of RTILs applications are wide-ranging and include organic and inorganic synthesis,[11] electrochemical studies,[12] nucleoside chemistry,[13] and physical chemistry studies.[10]

Solvation is the interaction between the solvent and solute. Often, applications of new technologies outpace fundamental understanding. Although one may successfully synthesize a compound using an IL solvent it would be helpful to know how the IL solvent solvates solutes. The gain is perhaps the ability to more specifically tailor the IL to enhance the desired synthesis. Solvation can be affected by, among other things, the polarity of the solute and solvent. If a solvent molecule is polar, it will respond to the electric field of a polar solute molecule and rearrange around the solute. Solute-solvent interactions always exist, but the relative strength of these interactions and also solvent-solvent, and solute-solute interactions are the real issue. Spectral shifts in a spectrum are a result of solvation and other factors. A dipole moment exists

as a natural consequence of electron arrangements. In nonpolar molecules the dipole moment is not as pronounced as in a polar molecule, so solvation is more difficult. In polar or charged groups, attraction to water creates property changes and therein solvation issues. An attractive feature of RTILs is that they are made of ions and therefore have desirable solvating properties such as the ability to dissolve a wide array of solute molecules. Depending on the cation and anion identity of the RTIL, highly polar to non-polar compounds can be dissolved. The structures of RTILs are the main factors affecting their properties including density and viscosity.[14] Viscosity depends on the cation or anion component of the RTIL.[10] Viscosity, along with other physical properties of RTILs, is influenced by the presence of water.[13] The phosphonium ionic liquid (PIL) is very viscous and can readily absorb water if not kept in a dessicator or closed system. Water is a very polar molecule and can easily affect the polarity, solubility, viscosity, and conductivity of a RTIL. The water molecules interact with the anion of the RTIL forming hydrogen or induced hydrogen bonds among water molecules.[15] A stronger interaction with the anion causes more water to be absorbed than with a weaker anion. There is always some water present in RTILs when they are exposed to air, although the amount of water depends on the structure of the RTIL. Absorption of water to the RTIL has been shown to significantly slow solvation dynamics.[16,17]

Imidazolium ILs are currently the most popular ILs studied. Imidazolium ILs are of interest because their solvation dynamics have a biphasic character with a fast and slow component.[1,18] The solvation dynamics of this IL class are related to the ring structure of imidazole and the N–H bond causing strong hydrogen bonding and a charged polar molecule. In imidazolium ILs the fast component of solvation was found to be caused by motions of the cation and anion, while the slow component is associated with structural rearrangement.[19] PILs

differ from imidazolium ILs in that they are very viscous and correlate to the slower component of the solvation response.[18] PILs also have a structure with long alkyl chains and no ring. This structure allows interactions between the chains creating a viscous solvent and therefore slower solvation response. The specific PIL used in this project was trihexyltetradecyl phosphonium chloride (RTPIL-Cl), Figure 1. Any number of technologies can be used to measure the solvent response to a stimulus. This work describes the use of a fluorescent molecule to probe the solvent environment of this PIL.

### 1.2 Fluorescence Spectroscopy

Fluorescence spectroscopy is an instrumental technique that uses photons to directly probe molecular interactions. Fluorescence is the emission of the probe when it drops in energy from the excited state to the ground state. An energy or Jablonski diagram in Figure 2 shows the transitions between excited and ground states, including fluorescence. The fluorescent probe absorbs photons from an excitation resulting in electron distribution. For fluorescence the photons are excited from the ground state to the first excited singlet state. The probe forms a dipole moment at this higher energy state due to the electron distribution and a shift in orientation. If energy relaxation is in the form of photons, they are emitted as the excited probe molecule returns to the energetically-favored ground state. There are several transitions that can occur in spectroscopy. Nonradiative transitions include internal conversion or intersystem crossing. Internal conversion is from the first excited singlet state to the ground state. Intersystem crossing can be from the excited singlet state to the excited triplet state or from the excited triplet state to the ground state. Intersystem crossing occurs between states of different spin multiplicity. Photon emission tends to be the dominant form of relaxation. This radiative decay process includes fluorescence and phosphorescence. Fluorescence is the radiative decay process

that occurs when a molecule transitions from the first excited singlet state to the ground state via photon emission between states of the same spin multiplicity.[20] Phosphorescence occurs when a molecule transitions from the first excited triplet state to the ground state via photon emission between states of different spin multiplicity. Fluorescence occurs with higher probability and at a faster rate than phosphorescence because there is no change in spin multiplicity.

In our experiments we looked at the fluorescence of the probe in neat and mixed systems, since molecular state depends on the molecular environment. The probe's fluorescence directly corresponds to the molecular interactions occurring in the solvent. The number of photons or energy released by the probe is presented in an emission spectrum.

The cybotatic region directly influences the emissive properties of the probe. This includes interactions between the solute-solvent, solute-solute, and solvent-solvent. The chemical environments in our experiments included a polar fluorophore, a RTPIL with a long alkyl chains and/or methanol. The interactions between the probe's excited state and the cation, anion and alkyl chains of the RTPIL all affect the fluorescence. These interactions are manifested in the probe's emission spectrum, which shows the intensity variation as a function of wavelength.

If one is measuring fluorescence, desirable probe features when include fluorescence, a dipole moment, and insensitivity to water on solvation. In general, the family of coumarin molecules is highly fluorescent and commonly used as blue-green laser dyes, optical bleaching agents, and in our case, fluorescence probes. Coumarin 153 (C153, Figure 3) is a highly dipolar solute[21] and is known for its sensitivity to solvent polarity.[22] Therefore C153 is ideal for measuring solvation dynamics, and although there is a small amount of water always associated with the RTPIL its presence here does not significantly impact the C153 emission spectra.[13]

Interactions in the cybotatic region of C153 are determined using fluorescence spectroscopy. In this work we used steady-state and time-resolved fluorescence to determine the molecular solvation of C153. Steady-state emission results from continuous illumination of the probe and gives a time-averaged characterization of the probe's emissive properties and response to bulk solvent properties or behavior. However, time-averaged data is somewhat limited in value because it is by definition an average response and contains no dynamic information. Therefore, any specific dynamical behavior is not detected and the details of solvation are largely washed out. In contrast, time-resolved emission measurements reveal the details of molecular dynamics and it is this data that provides the critical information to more completely understand the details of solvation. Pulsed illumination of the probe allows measurement of the emission intensity decay, which depends on the time that the probe remains in the excited-state. This is the lifetime of the probe. Emissive times are typically near $10^{-8}$ seconds.

Subsequent to electronic excitation, C153 undergoes a large change in polarity. C153 interacts with the surrounding solvent and eventually reaches equilibrium within a few nanoseconds.[23] Solvent equilibrium depends on the solute-solvent interactions, polarity, energy, water present, viscosity and other interactions in the solution. Solvents currently studied include RTILs, supercritical fluids, organized media (micelles), solid surfaces (silica) and mixed systems.[24] The solvents used in our experiments were RTPIL, MeOH, and RTPIL-MeOH mixed systems.

### 1.3 Solvation Dynamics

Solvation dynamics encompasses several phenomena that depend on specific solute interactions with a solvent, one of which is the rate of solvent reorganization.[25] Solvation stems

from the structural rearrangements that a solvent undergoes to accommodate a solute molecule, and directly corresponds to the instantaneous energy of the system, as seen in Figure 4. When the solute molecule reaches the excited state, its dipole moment induces the solvent to reorganize to a more energetically favored arrangement. The time it takes for solvent reorganization or relaxation around the probe is the solvation time. Solvation dynamics allow understanding of the overall polarity of the probe and not specific interactions, like hydrogen bonding and dispersion.[24] The solvation time is affected by the solute's molecular structure, the solvent environment, i.e. polar and nonpolar solvents, and temperature.[5,26,27,28,29,30] Solvation can also be affected by impurities like water or any other chemical systems.[31] Solvation dynamics of RTILs are influenced by all of the above. RTILs have unique solvating characteristics with a slower solvent equilibration as compared to most conventional polar solvents.[32] This is not surprising given their high viscosities, structures and heterogeneity.[16] High viscosity was also shown to cause slow rotational relaxation.[19] Experiments comparing the various RTILs, suggest that solvation dynamics of RTILs are primarily influenced by cation motions. This is because of the large solvation differences between PILs and imidazolium ILs.[1] There are also variations in instrumentation and methologies that cause differences in reported solvation times.[31]

Solvation dynamics are commonly studied using time-resolved fluorescence.[10] By understanding the time scale of solvent reorganization one can learn to tailor RTIL solvent to carry out reactions for a desired product.[5] However, careful consideration must be given to solute-solute, solvent-solvent and solute-solvent interactions.

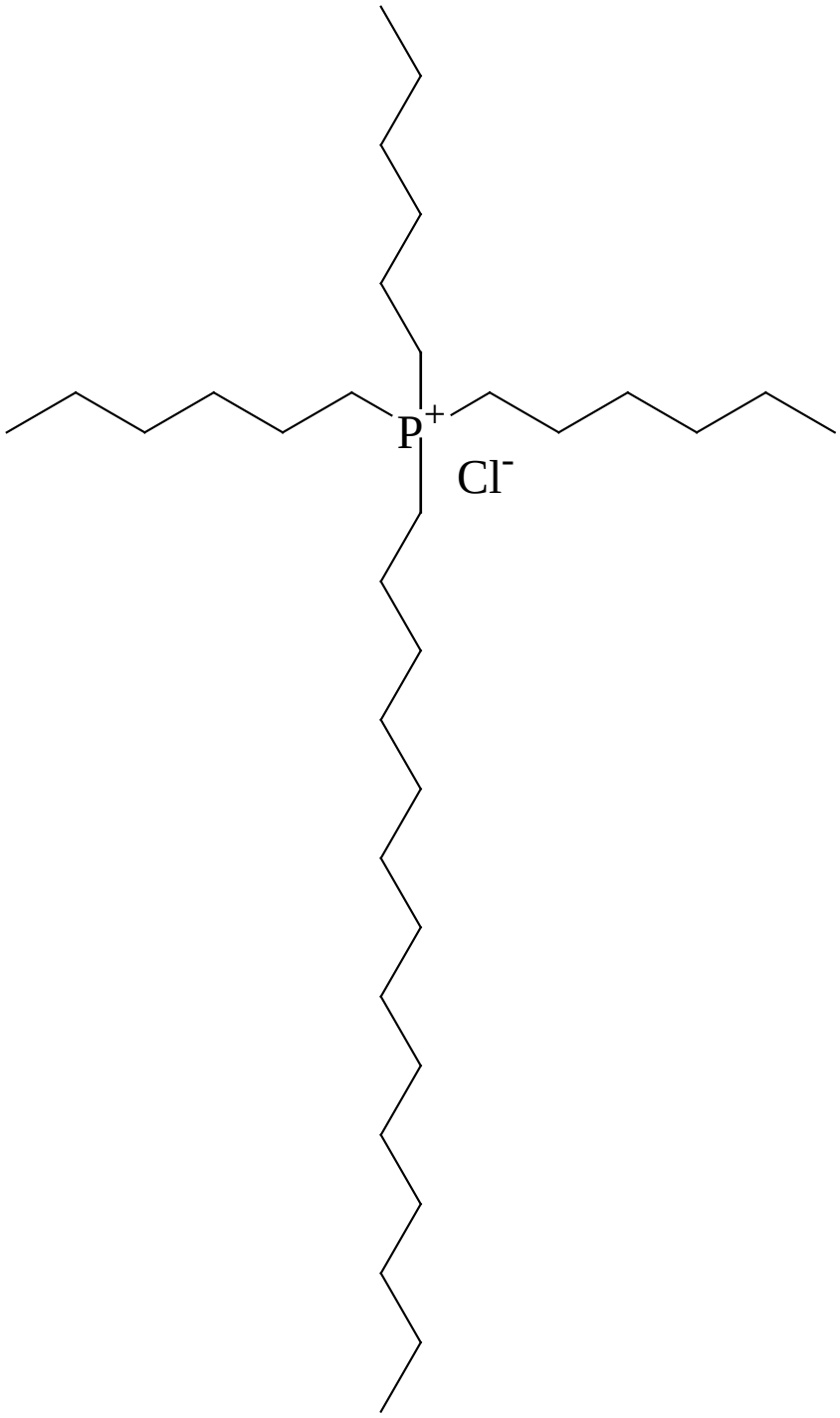


**Figure 1.** The chemical structure of trihexyltetradecyl phosphonium chloride (RTPIL-Cl).

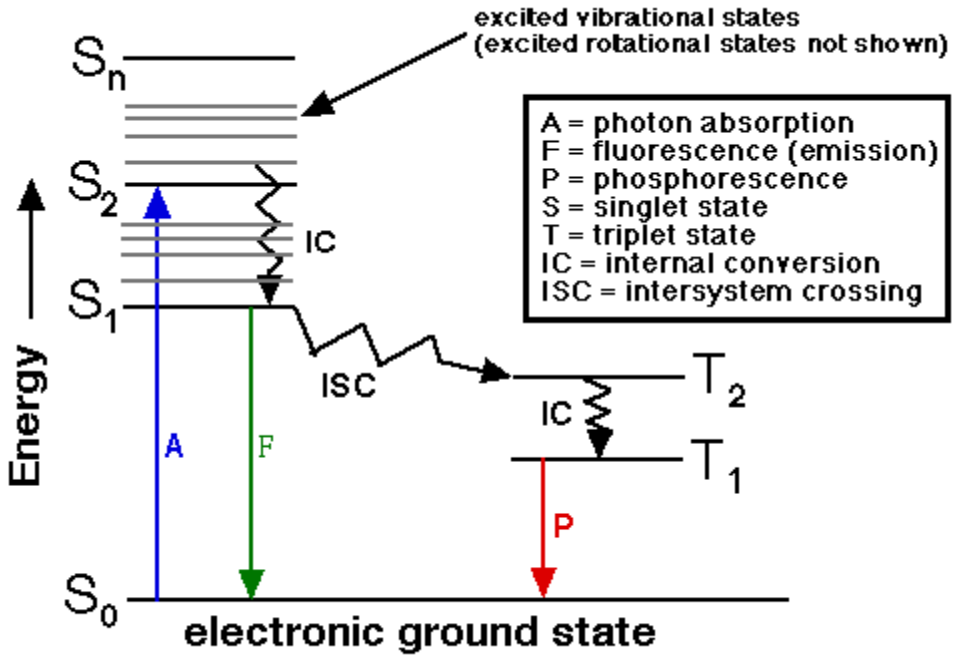


**Figure 2.** The Jablonski diagram shows the photons transition from the ground state to the excited states and back to the ground state. Photons are absorbed, shown as a blue line, resulting in a higher energy state. There are several ways the photons relax back to the energetically-favored ground state. Internal conversion is a nonradiative transition from one state to another lower energy state. Intersystem crossing is also a nonradiative transition and is shown from the singlet state to the triplet state. The spin multiplicity is changed in intersystem crossing. Fluorescence, shown as a green arrow, is a radiative transition from an excited singlet state to the ground state. Phosphorescence, shown as a red arrow, is also a radiative transition, but from an excited triplet state to the ground state and also results in a change in spin multiplicity. Fluorescence is a faster process than phosphorescence because there is no change in spin multiplicity.

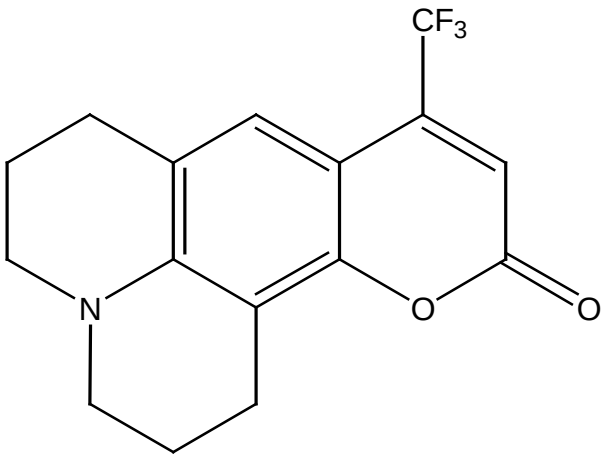


**Figure 3.** The solute or fluorescent probe, coumarin 153 (C153). Its emissive properties directly relate to the environment around the probe.

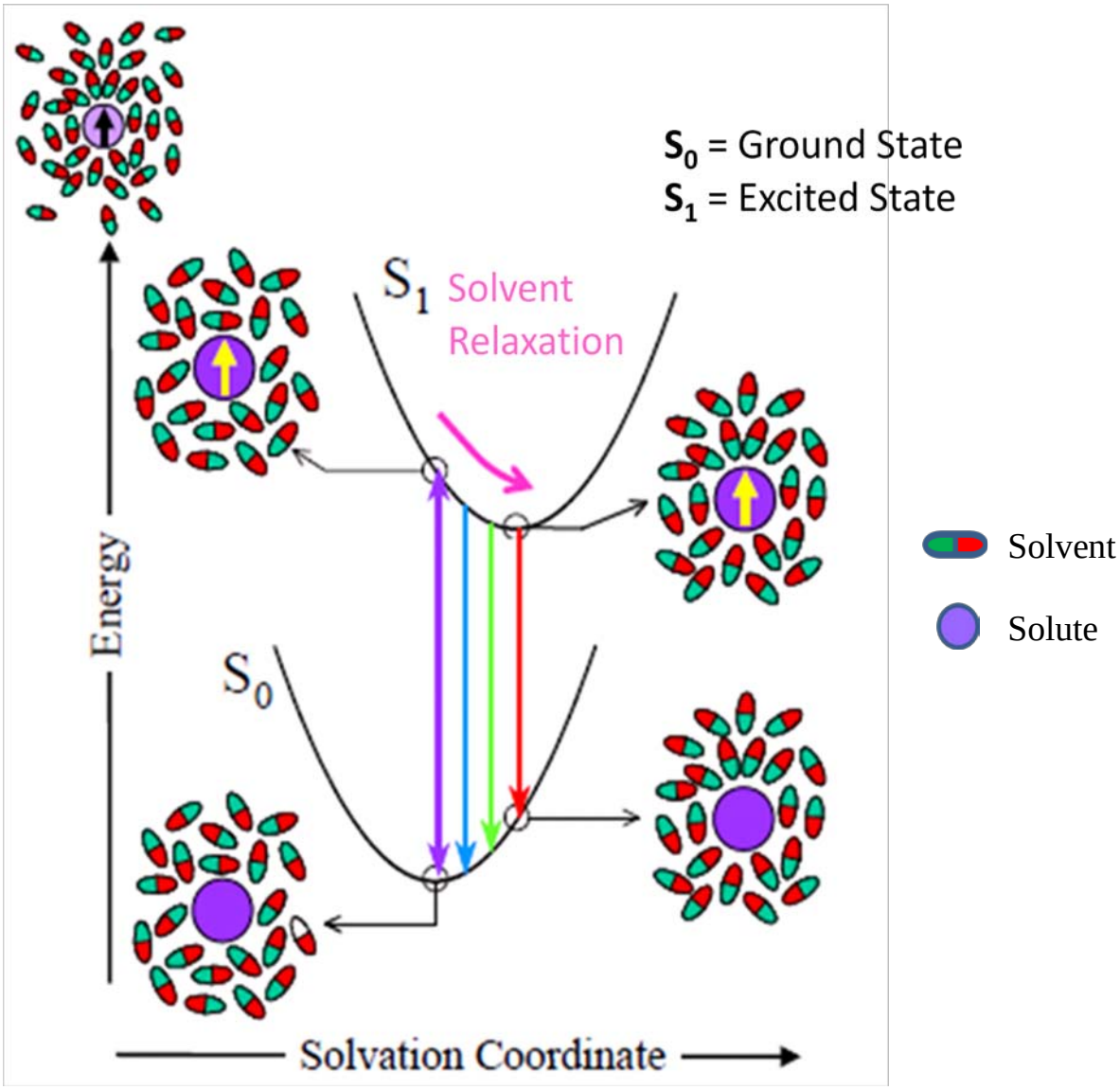


**Figure 4.** The solvent in this project was MeOH, RTPIL-Cl, or MeOH/RTPIL-Cl mixed systems. The solute was the probe C153. The solvent molecules have a dipole movement, as seen by the red and green ends. The solute when excited has a dipole movement shown as a yellow arrow. Solute-solvent interactions can be seen by the solvent arrangement around the probe. Solvent relaxation causes a decrease of energy in the excited state and the solvent molecules rearrange into a more favorable formation. The solute drops back into the ground state at various periods of relaxation and energy as shown by the purple, blue, green and red arrows.

# Chapter 2

## Experimental

RTPIL-Cl was donated by Cytec, Inc. and used as received. C153 was bought from Exciton, Inc. and used as received. HPLC grade MeOH was bought from Fisher Scientific and also used as received. Standard 1 cm path length quartz fluorescence cuvettes were thoroughly cleaned in dilute nitric acid solution, rinsed with hot tap water followed by copious rinsing with distilled-deionized 18.3 MΩ water, and finally rinsed several times with HPLC grade MeOH and then left to dry. All C153-containing solutions were prepared from a ~1 mM stock C153 solution. The stock C153 solution was prepared by dissolving 1.6 ± 0.0001 mg C153 in 3.4 mL MeOH. Samples were made such that the final C153 concentration was between 1 and 10 μM C153. Absorbance measurements (not shown) verified that the optical density (O.D.) of all C153 solutions was less than 0.1 O.D. at 420 nm excitation. To prepare a sample for measurement, we first added the stock C153/MeOH solution to an empty cuvette and the MeOH was evaporated with a gentle stream nitrogen gas. Two milliliters of MeOH was added to the cuvette to make the "base" MeOH solution. To this solution, successive masses of IL were added to create the desired mol fraction IL solution. All IL additions required that we measured mass because the viscosity prevented the use of micropipetters. Similarly, to prepare a solution on the bulk IL side of the mol fraction scale ($x_{il} > 0.13$) we started with an initial C153/IL solution to which a calculated number of moles MeOH was added to produce the desired mol fraction solution. The solution of bulk IL was prepared using approximately 3 g IL and 10 μL C153/MeOH.

To prepare a desired mol fraction solution the density of MeOH was used to calculate the number of moles needed to make the solution and the corresponding volume of MeOH was pipetted. The IL was added last and air bubbles formed in the cuvette because the IL is very

viscous. The C153/IL mixed system was heated for 2 minutes in a 110 $^{o}$C oven to allow the system to mix and get rid of air bubbles. The cuvette was inverted several times to mix the solution until the diffraction gradients were gone. To this solution varying amounts of MeOH was added to recreate the mol fractions, shown in Table 1. In the same way, a solution of bulk MeOH was prepared with 3.0 mL MeOH and 10 µL C153/MeOH using a Gilson pipette. By mass difference, RTPIL-Cl was added to the cuvette to obtain the desired mol fractions, shown in Table 1.

Absorption data was measured with a Perkin-Elmer Lambda 800 UV/Vis Spectrometer from 250-550 nm. The parameters were set to a scan rate of 60 nm per minute and the bandpass was 2 nm. Steady-state and time-resolved fluorescence data was measured using a Horiba Jobin-Yvon SPEX Fluorolog-3 MHF (multi-harmonic frequency) domain spectrometer. For steady-state fluorescence, the sample was excited at 420 nm and the emission spectrum was taken from 435 to 700 nm in 1 nm increments. The excitation and emission bandpasses were set at 2 nm and the integration time was at minimum 0.2 seconds. The emission was corrected for grating effects using a correction file supplied by SPEX and ratioed to the lamp intensity to correct for any lamp fluctuations during the measurement.

For the time-resolved fluorescence measurements, the data was collected at various emission wavelengths using long pass and band pass filters. Filters included a 450 nm long pass, and band pass filters of 458, 480, 500, 515, 532, 550, 568, and 610 nm. For time-resolved data collection, the lights to the room were turned off to prevent stray light from affecting the measurements. Data was acquired until the phase error was either less than 0.5$^{o}$ or had a relative standard deviation of no more than 0.10 or reached a maximum of 10 replicates.

The software program DATAMAX was used to model the lifetime data (intensity decay). Discrete functions were used including a first, second and third exponential. Discrete functions are the sums of exponentials to create a continuous function.

**Table 1. Summary of Mol fractions Ionic Liquid**

| bulk MeOH phase[a] | | | | | | |
|---|---|---|---|---|---|---|
| mass Cl (mg) | V (μL) ilcl[b] | mmol Cl | x(ilcl) | x(meoh) | mass fr ilcl | V fr ilcl |
| 0.0 | 0.00 | 0.000 | 0.000 | 1.000 | 0.000 | 0.000 |
| 8.1 | 8.93 | 0.016 | 0.000 | 1.000 | 0.005 | 0.004 |
| 35.3 | 38.91 | 0.068 | 0.001 | 0.999 | 0.022 | 0.019 |
| 94.1 | 103.72 | 0.181 | 0.002 | 0.998 | 0.056 | 0.049 |
| 209.9 | 231.35 | 0.405 | 0.005 | 0.995 | 0.117 | 0.104 |
| 303.1 | 334.07 | 0.585 | 0.008 | 0.992 | 0.161 | 0.143 |
| 591.5 | 651.94 | 1.141 | 0.015 | 0.985 | 0.272 | 0.246 |
| 1049.1 | 1156.30 | 2.023 | 0.027 | 0.973 | 0.399 | 0.366 |
| 1149.7 | 1267.18 | 2.217 | 0.056 | 0.944 | 0.421 | 0.388 |
| 1756.9 | 1936.43 | 3.388 | 0.103 | 0.897 | 0.526 | 0.492 |
| 1815.8 | 2001.34 | 3.502 | 0.124 | 0.876 | 0.534 | 0.500 |

| bulk ionic liquid phase[a] | | | | | |
|---|---|---|---|---|---|
| V (μL) meoh | mmol meoh[b] | x(ilcl) | x(meoh) | mass fr ilcl | V fr ilcl |
| 1000.0 | 24.719 | 0.133 | 0.867 | 0.752 | 0.714 |
| 639.0 | 15.795 | 0.263 | 0.737 | 0.826 | 0.796 |
| 426.0 | 10.530 | 0.349 | 0.651 | 0.877 | 0.854 |
| 213.0 | 5.265 | 0.517 | 0.483 | 0.934 | 0.921 |
| 0.0 | 0.000 | 1.000 | 0.000 | 1.000 | 1.000 |

[a]A bulk MeOH phase means that the masses of ionic liquid reported in this table were added to an initial 2000 μL C153/MeOH solution. Similarly, the ionic liquid rich side of the mixtures was prepared by filling the cuvette with an initial mass of 3000 mg IL. To this mass MeOH volumes were added using a micropipetter.

[b]Volume or mass, as appropriate, were calculated from the reported densities, 0.9073 g-mL$^{-1}$ for the IL[33] and 0.791 g-mL$^{-1}$ for MeOH[34].

# Chapter 3

## Results and Discussion

### 3.1 Steady-State Emission

We measured the steady-state emission of C153 as a function of mol fraction of PIL-Cl in MeOH. The solutions, shown in Table 1, were always single-phased and optically transparent at all mol fraction compositions. Steady-state spectra were in general broad and featureless. The C153 emission spectra showed a systematic blue shift from MeOH-rich to PIL-Cl rich. As the solutions became richer in ionic liquid there was a marked decrease in emission intensity, which passed through a minimum. Figure 5a shows a plot of the spectra intensities. In the MeOH-rich system the C153 intensity was $2.8 \times 10^7$ counts per second (cps) and the observed $\lambda_{max}$ was 530 nm. The presence of ionic liquid, even at the lowest mol fractions, immediately influenced the emissive properties of C153. The concomitant blue shift and decreased intensity continued until a mol fraction of about 0.03, at which point the emission intensity began to increase. At the PIL-rich end we note that the intensity peaked at $2.4 \times 10^7$ cps, very nearly the same as the C153/MeOH solution. However, the $\lambda_{max}$ was observed at 500 nm. This behavior clearly indicates that the net energy of the system is greater in a purely ionic liquid solution as compared to a neat MeOH solution. This may be a bit counter intuitive given that one would expect an ionic solution to readily solvate a highly polar molecule and to provide a solvent environment that accommodates such a molecule. One notable point here is that the presence four alkyl tails on the phosphonium cation creates a region of hydrophobicity in which C153 would certainly couple less strongly. This is consistent with simple C153/solvent solutions in which C153 is dissolved in nonpolar or aprotic systems, e.g., cyclohexane or dmf. The emission in these systems is also significantly blue shifted relative to emission in MeOH[13] (also measured in-

house, data not shown). The normalized data is shown in Figure 5b. The systematic progression of the emission maximum shows a steady blue shift with a more pronounced effect in the ionic liquid rich solutions. The rate of change is slower in the MeOH-rich solutions than the PIL-rich solutions. There were more additions of PIL to the MeOH-rich solutions, while the PIL-rich solutions had few additions of MeOH and the mol fractions were more spread.

To more fully describe the observed steady-state emission we plotted the spectral peak wavelengths, widths, and intensities. To directly relate the emission peak wavelength to energy the spectra were converted to frequency in $cm^{-1}$. Spectral widths were characterized by calculating the full width at half maximum of the normalized spectrum. The values of peak frequency, intensity, and full width at half maximum (FWHM) were calculated using an in-house software program. To enhance the clarity of the plot, all of the data was plotted as a function of the logarithm of mol fraction PIL-Cl because the IL additions in the MeOH rich solutions were small enough that the data is too compressed to easily differentiate. Figure 6a shows the relative energy of C153 in mol fraction is varied. Small amounts of PIL added to a bulk MeOH solution do not appear to perturb the solvation of C153, since the emission frequency does not change significantly. In contrast, the energetics do show a distinct change at PIL mol fractions greater than log mol fraction PIL of -1.0 (= 0.1 $x_{cl}$). To contrast the MeOH-rich and PIL-rich solutions, the break in slope was estimated by eye and the slopes for each end calculated. The slope changes by nearly a factor of two, from 0.044 in MeOH-rich solutions to 0.74 in PIL-rich solutions (in this case <0.1 $x_{cl}$), although there is no distinct break per se in this data. Panel (b) shows the variation of peak intensity as PIL is added. Two points are noteworthy here. First, the MeOH solution showed a slightly greater intensity with an approximately 23% increase in intensity over the PIL solution. Second, the intensity has a pronounced minimum at a log PIL

mol fraction of -1.5 as compared to the peak position data. We interpret the minimum in emission intensity as a quenching of C153, around a mol fraction PIL of 0.03. It is interesting to note that the dip in intensity occurs at roughly the same mol fraction as the change in slope of the peak position. These points taken together begin to present a consistent picture of the influence of the mixed system on C153 solvation. We also plot the FWHM, shown in Figure 6c. FWHM provides some insight regarding solution homogeneity. Upon inspection of the full width data, panel (c) displays a very distinct change in slope at log PIL mol fraction greater than -1.0 or mol fraction PIL of 0.1. The change in slope was estimated by eye, so that PIL-rich solutions were $<0.1\ x_{cl}$. The slope changes from 0.016 ± 0.004 in MeOH-rich to 0.32 ± 0.02 in PIL-rich solution. The slope changes by a factor of 20 from MeOH- to PIL-rich solutions. This is a very significant change and illustrates that C153 interacts differently in MeOH than in PIL. This observed change in FWHM is consistent with the other spectral parameters.

To summarize, the steady-state emission data show that solvation of C153 is at a greater net energy in PIL than MeOH. The blue shift in the emission spectrum and the peak frequency both show the solvation energetics of C153 continually increase going from a neat MeOH to neat PIL solution. The cybotatic region about C153 in the ionic liquid is clearly different than in MeOH. This may be due to the hydrophobic chains of the PIL forming micelles and affecting the probe environment. PIL have long alkyl chains versus the short $CH_3$ group on MeOH. The probes environment becomes more complicated in the long alkyl chains making the solvation energetics greater. Also strong hydrogen bonding in MeOH can cause little interaction between MeOH and the probe, so solvation energetics are less. There is possible solute-solute interactions causing aggregation and affecting the emission spectrum, but this is very unlike at the small concentration of C153 we used. The peak intensity suggests quenching of C153 at a PIL mol

fraction of 0.03. Finally the FWHM shows solvation changes of C153 in PIL versus in MeOH. The energetics of the system change drastically at PIL mol fractions greater than 0.1.

### 3.2 Time-Resolved Fluorescence

Time-resolved intensity decay measurements were collected for C153 at the same mol fractions of PIL as reported for the steady-state measurements to probe the C153 solvation dynamics. Time-resolved data gives more detailed information about the emissive behavior of C153 and in particular allows us to characterize time-dependent molecular events that occur during the excited-state lifetime of the probe. In particular, we were interested to determine how the C153 excited-state responds to solvent reorganization as the composition of solution is changed. To map out the time course of solvation (Figure 4), we need to collect time-resolved emission data at various points across the C153 emission spectrum. A 450 long pass filter collected time-resolved data for the entire emission spectrum of C153 for each mol fraction. A 450 long pass filter allows photons to pass after a wavelength of 450 nm. Since the emission spectrum of C153 occurs at wavelengths greater than 450 nm, the long pass filter collects time-resolved or intensity decay data for the entire spectrum. This intensity decay of C153 is an average for each emission spectrum. Seven 10 nm FWHM bandpass filters were used to dissect the emission spectrum at each mol fraction and time-resolved emission spectra were constructed from these data. The bandpass filters used in these experiments had wavelengths centered at 480, 500, 515, 532, 550, 568, and 610 nm. Although the steady-state emission varied significantly as mol fraction changed, these filters adequately covered the entire emission spectrum at all mol fractions. By dissecting the emission spectrum in this way, the complete solvation surface can be defined and the solvent relaxation determined.

The (excited-state) lifetime is defined as the amount of time the probe spends in the excited state before returning to the ground state. The C153 lifetime (<*t*>) was calculated from the intensity decay data using Equation 1:

$$\langle t \rangle = \frac{\sum_i t_i N_i(t)}{\sum_i N_i(t)} = \frac{\int_0^\infty tN(t)dt}{\int_0^\infty N(t)dt} = \frac{\int_0^\infty te^{-t/\tau}dt}{\int_0^\infty e^{-t/\tau}dt} \qquad \textbf{eqn. 1}$$

where *t* is time, *N(t)* is the intensity at time t, and $\tau$ is the excited state lifetime. The intensity decays were fit to single, double, and triple exponential models using a non-linear least squared fitting routine based on the Marquardt-Levenberg algorithm. The lifetime and pre-exponential factors were allowed to freely vary in the models and the best fit to the data was judged by the reduced chi-squared value ($\chi_r^2$). The average lifetime was determined for each mol fraction at each bandpass. A double exponential model had a better fit for the lower wavelength bandpass data, while for the higher wavelengths were best described by a single exponential model. As expected based on literature reports, the intensity decay of C153 in neat MeOH (with no PIL added) resulted in a single exponential model as the best fit, consistent with the idea that MeOH is a simple system and shows no anomalous behavior. With PIL added however, the system becomes inherently more complex and viscous, and data from solutions with mol fractions PIL greater than 0.10 required a double exponential model to describe the intensity decay. We did test all data sets with a triple exponential model but in no case was there a significant improvement in the $\chi_r^2$ that would warrant using a more complicated model. The best models for each mol fraction and bandpass is shown in Table 2.

To begin, we compared this new set of intensity decay data collected using a 450 nm longpass filter to data acquired in preliminary experiments (2008) and found excellent agreement between the data sets, see Figure 7. The comparison confirmed at least two things: 1) the instrument is producing consistent data and it is highly reproducible; and 2) the ionic liquid is

very stable when stored over desiccant over long periods of time. However, what is particularly important is that both data sets showed a minimum value in the recovered C153 lifetime at a mol fraction of 0.03 (log mol fraction = -1.5). The quenching of fluorescence at this mol fraction clearly demonstrates that the solute-solvent interactions are uniquely different than in either neat solvent alone. Inspection of the data shows that in the PIL-rich solutions the trend in recovered lifetimes is somewhat more scattered. We attribute this to the method of sample preparation for PIL-rich solutions. It was more difficult to prepare these solutions because the high viscosity of the IL required that we heat in order to ensure that a homogeneous solution resulted.

Consistent with the chemical literature, we observe that the excited state intensity decay is complex and likely contains more information than we are capable of resolving with our present instrumentation. Rather than attempting to ascribe specific physical features of the chemical system to a particular fitting component, the intensity decay is characterized as a simple weighted-average of the lifetime components. Figure 8 displays the weighted average of lifetime (ns) versus log ($x_{cl}$) at each emission wavelength. Panel (a) is the data collected at the blue edge of emission (480 nm) and panel (g) is the red edge of emission (610 nm). It is clear to see in these data that, regardless of emission wavelength, a distinct minimum in the recovered lifetime is observed at approximately the same mol fraction IL. Upon closer examination of the data several features are of note. First, the average lifetime from MeOH- to PIL-rich changed for each bandpass. At the blue edge of emission (480 nm) the average lifetime does not change much at the extremes, but shows a slight dip in the lifetime. Using the red edge emission (610 nm), we observe that the average lifetime changes more dramatically across the complete range of mol fraction, from a lifetime of 4.0 ns in MeOH to 6.0 ns in PIL. The differences in lifetimes between MeOH- and PIL-rich solutions are small at 480 and large at 610 with the other

bandpasses' lifetime differences falling in between these extremes. For both the MeOH- and PIL-rich solutions, the lifetime increased as the bandpass increased. For example, from a 500 bp filter to a 532 bp filter the minimum lifetime increased from around 2.65 ns to 2.75 ns. This change in lifetime is not very significant in MeOH-rich solutions, but was more drastic and significant in PIL-rich solutions. We attribute all these changes to solvent structure differences. MeOH has a simple hydrogen bonding network and weak van der Waals interactions between the methyl groups and in contrast the PIL has a much more complex structure that depends on ion-ion interactions as well as stronger van der Waals interactions between the longer alkyl chains. At a minimum, the solvent-solvent interactions and high viscosity of the PIL are responsible for the relative complexity of solvation in PIL/MeOH solutions. Therefore, the reorientation kinetics of PIL would be more complicated and the lifetimes are expected to change more dramatically.

To more clearly demonstrate the effect of bandpass and mol fraction a summary of all the bandpass data is plotted in Figure 9. C153 lifetime in MeOH and MeOH-rich solutions showed less variance in average lifetime, than C153 in PIL-rich solutions. The lifetime in PIL-rich solutions changed by approximately 2.0 ns whereas on the MeOH-rich side the difference was only 0.2 ns from the 480 to 610 nm bandpass. The average lifetime of C153 in pure MeOH was 4.30 ± 0.04 ns, while in pure PIL was 5.1 ± 0.6 ns. These lifetimes were an average of all the lifetimes at each bandpass in pure MeOH and pure PIL solutions. There is a larger relative standard deviation in PIL-rich solutions due to the viscous nature of PIL and large difference in lifetimes. RTPIL-Cl has a large absolute difference in average lifetime across the range of emission bandpasses and in general is longer lived at all emission wavelengths. PIL-Cl has very long chains around the positive phosphorous atom, so C153 shows more difficulty in interacting

with PIL-Cl versus with the simple structure of MeOH. The structure of the solvent is important, affecting solvation, viscosities, and densities.[14,32] Recent papers show that solvation times correlate directly to solvent viscosity.[8,32] Solvation is about 5-fold slower in PILs than imidazolium ILs of similar viscosity, suggesting the structure and motions of the cation are the primary determinants of solvation time.[1] To characterize the solvation response of C153 in the MeOH/PIL system, we calculated the time-resolved emission center of gravity and the solvation correlation function. The time-resolved emission center of gravity, $\bar{\upsilon}_{em,\,COG}$ (t), is proportional to the average energy of emission and is shown in **e**quation 2:

$$\bar{\nu}_{em,COG}(t) = \frac{\sum_{\lambda} I'(\lambda,t)\lambda^{-1}}{\sum_{\lambda} I'(\lambda,t)} \qquad \textbf{eqn. 2}$$

where *I'* is intensity at a specific wavelength, $\lambda$, at time, *t*. The solvation correlation function, *C(t)*, is the amount of time the probe takes to solvate in a solution. The function is shown in equation 3:

$$C(t) = \frac{\nu(t)-\nu(\infty)}{\nu(0)-\nu(\infty)} \qquad \textbf{eqn. 3}$$

where *v(t)*, *v(∞)*, and *v(0)* are the peak frequencies at time t, infinity, and zero, respectively. Figure 10 shows center of gravity in panel (a) and the solvation correlation function results in panel (b).

The emission center of gravity shows the solvent reorganization in terms of time (ns) for selected mol fractions in panel (a). At larger mol fractions of PIL the time evolution of C153 is long and therefore solvent reorganization is slower. At 0.015 mol fraction PIL the spectrum is completely relaxed in a few hundred ps. In contrast the relaxation is substantially longer at 0.517 mol fraction PIL, and on the order of ~5 ns. At the very least this behavior can be understood in the context of solvent viscosity. PILs have notably high viscosities around 1,000 cP at room temperature. PIL-Cl has very high viscosity of about 1750 cP at 25°C, about 3.5 times more

viscous than imidazolium ILs, which have viscosities of around 500 cP. The solvation correlation function in panel (b) shows that in PIL-rich solutions C153 solvates over a longer time, near 10 ns before the correlation is completely lost. This is consistent with the longer observed lifetimes of C153 in PIL rich solutions. Taken together, all of the data we have collected point to the same conclusion, that the solvation of C153 significantly slower in the PIL. However, what is rather interesting about the correlation data is that although the 0.015 mol fraction is predictably much less viscous, essentially that of neat MeOH, the correlation time at this mol fraction is similar to the PIL rich solution. Moreover, the correlation time that shows the most rapid alignment of solvent is observed at 0.124 mol fraction, near where the minimum occurs in the lifetime data. Ion-ion interactions and van der Waals forces cause the solvent reorganization around C153 to be much slower in PIL. Although MeOH has strong hydrogen bonding, that alone does not significantly impact the solvent reorganization.

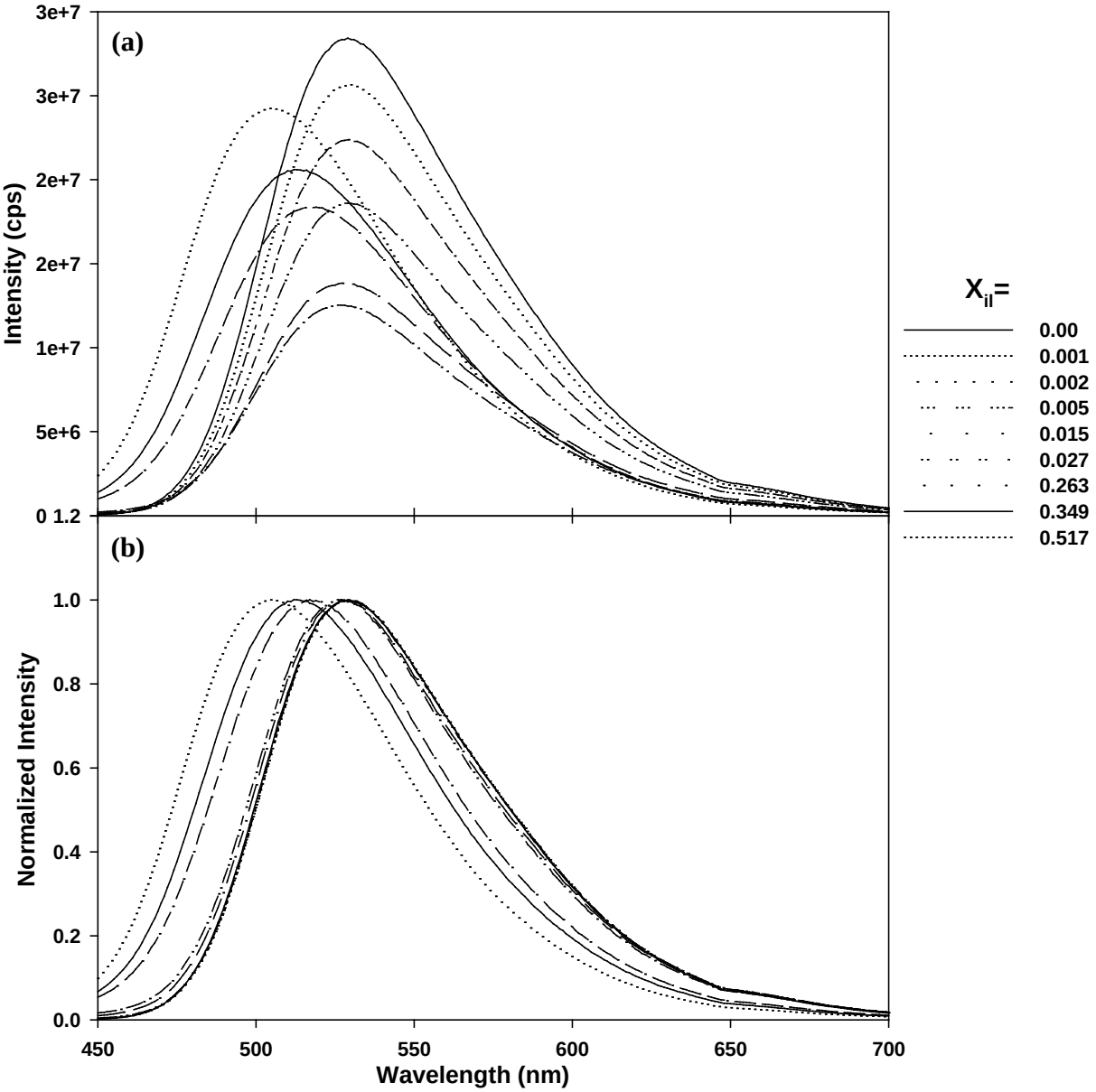


**Figure 5.** Steady state emission spectra of C153 in PIL-Cl/MeOH mixed systems. (a) Intensity versus wavelength and (b) the normalized intensity versus wavelength. There is a blue shift as RTPIL-Cl is added to the solution. C153-RTPIL interactions are less favorable as compared to C153-MeOH, since the system is at net higher energy in the PIL-rich solutions.

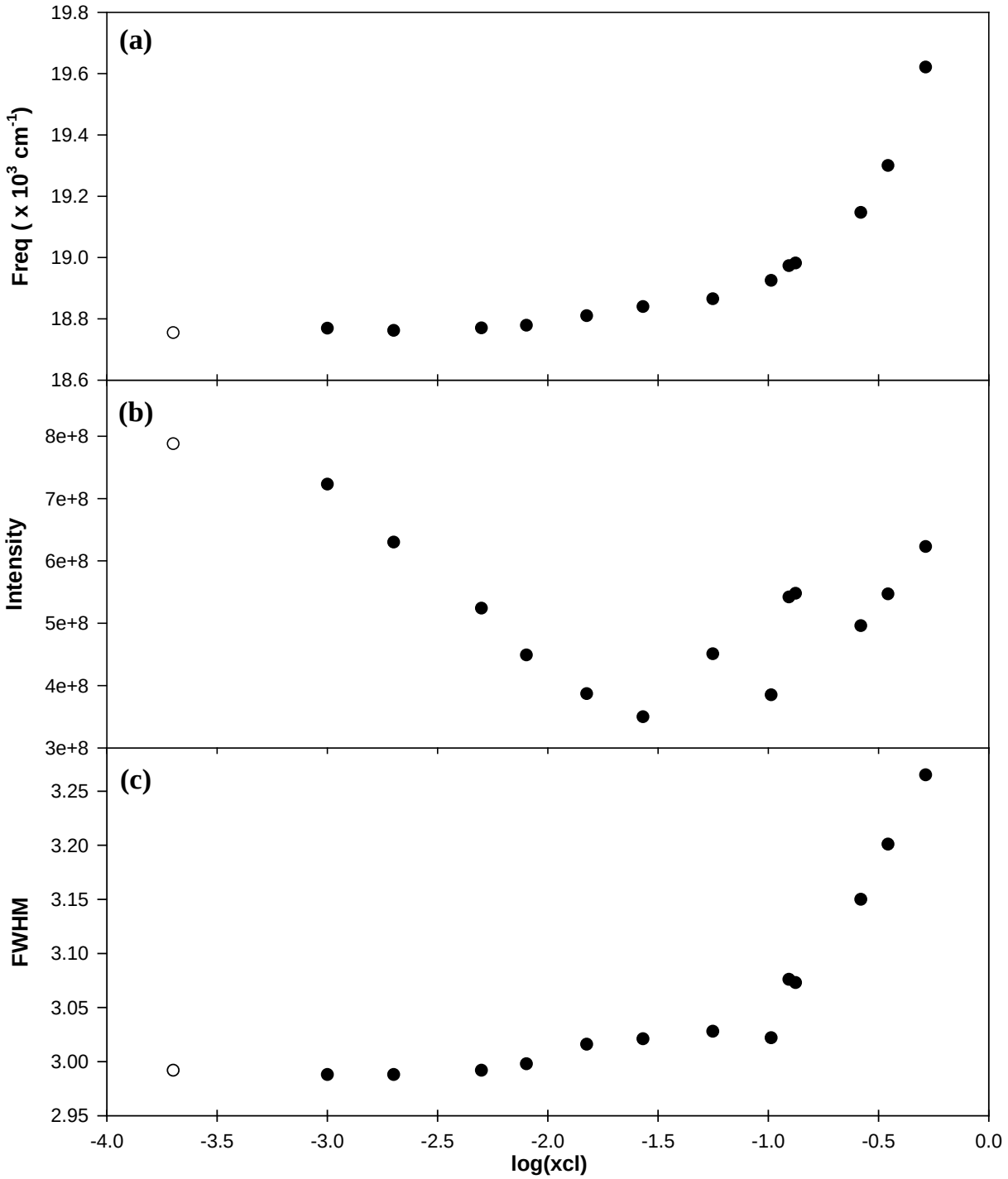


**Figure 6.** (panel a) Integrated area of the spectrum normalized versus logarithm of mol fraction of PIL-Cl [log ($x_{cl}$)]. (panel b) Peak frequency versus log ($x_{cl}$). (panel c) Full width at half max (FWFM) versus log ($x_{cl}$). All graphs are in terms of frequency instead of wavelength. MeOH-rich solutions are towards the left ($x_{cl}$ = -4.0) and PIL-rich solutions towards the right of the graphs ($x_{cl}$ = 0.0).

**Table 2.** Best Fit Models for each Mol fraction Solution

| x(ilcl) | Emission Wavelengths (nm) | | | | | | |
|---|---|---|---|---|---|---|---|
| | 480 | 500 | 515 | 532 | 550 | 568 | 610 |
| 0.0000 | s | s | s | s | s | s | s |
| 0.0002 | s | s | s | s | s | s | s |
| 0.0010 | s | s | s | s | s | s | s |
| 0.0020 | s | s | s | s | s | s | s |
| 0.0050 | s | s | s | s | s | s | s |
| 0.0080 | s | s | s | s | s | s | s |
| 0.0150 | d | s | s | s | s | s | s |
| 0.0270 | d | d | d | s | s | s | s |
| 0.0560 | d | d | d | s | s | s | s |
| 0.1030 | d | d | d | d | s | s | s |
| 0.1240 | d | d | d | d | s | s | s |
| 0.1330 | d | d | d | d | s | s | s |
| 0.2630 | d | d | d | d | s | s | s |
| 0.3490 | d | d | d | d | s | s | s |
| 0.5170 | d | d | d | d | s | s | s |
| 1.0000 | d | d | d | s | s | s | s |

[a]The fitting codes are "s" represents a single exponential decay model and "d" is a double exponential decay. The fits are the judged by the values of $\chi_r^2$.

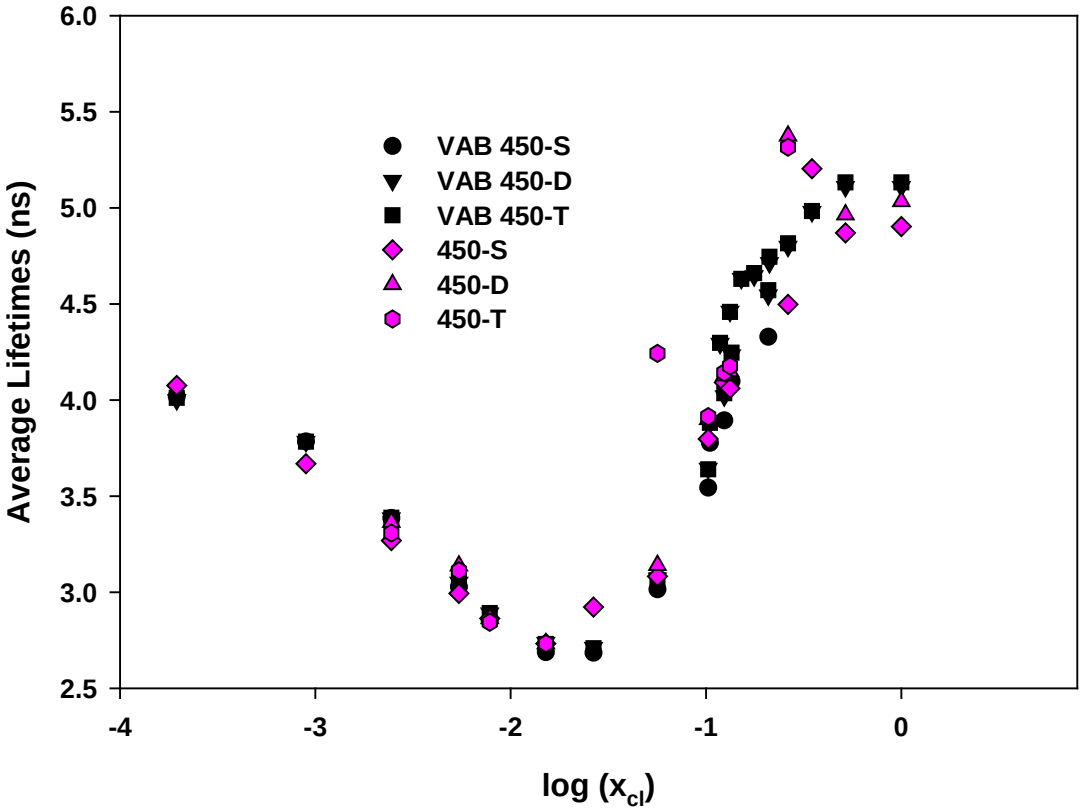


**Figure 7.** Comparison of lifetime data for MeOH/IL mixtures. Weighted-average lifetimes (ns) were measured using a 450 long pass filter to acquire the data. "VAB" symbols are data that were measured in 2008. "450" symbols are data collected in these experiments.

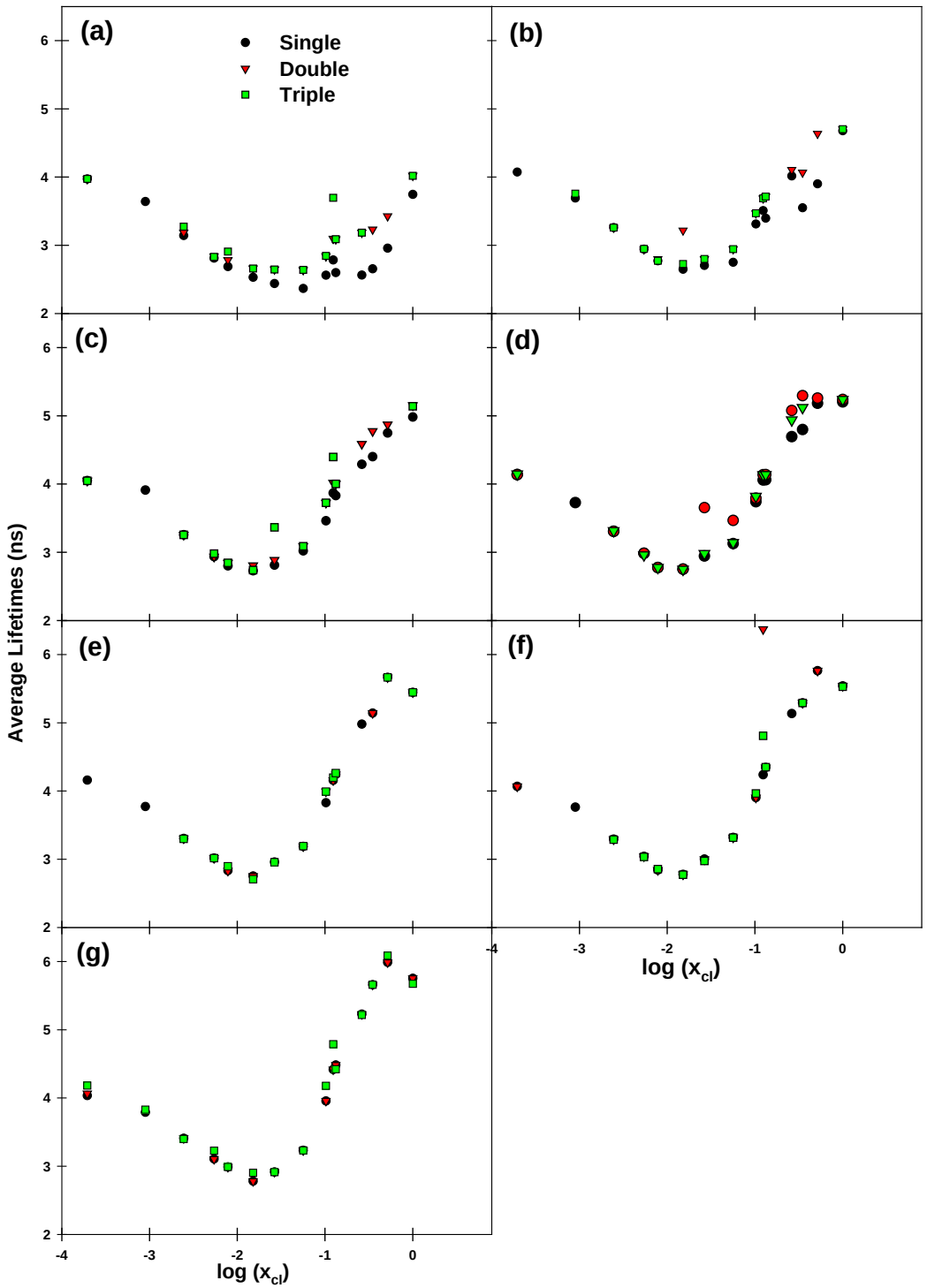


**Figure 8.** Weighted-average lifetime (ns) for each band pass filter: (a) 480 bp (b) 500 bp (c) 515 bp (d) 532 bp (e) 550 bp (f) 568 bp (g) 610 bp. Shown are fits to a single exponential decay model (●), and the lifetimes were recovered using Globals Unlimited®. Also shown are the average lifetimes recovered using a double exponential model (▼), and a triple exponential model (■).

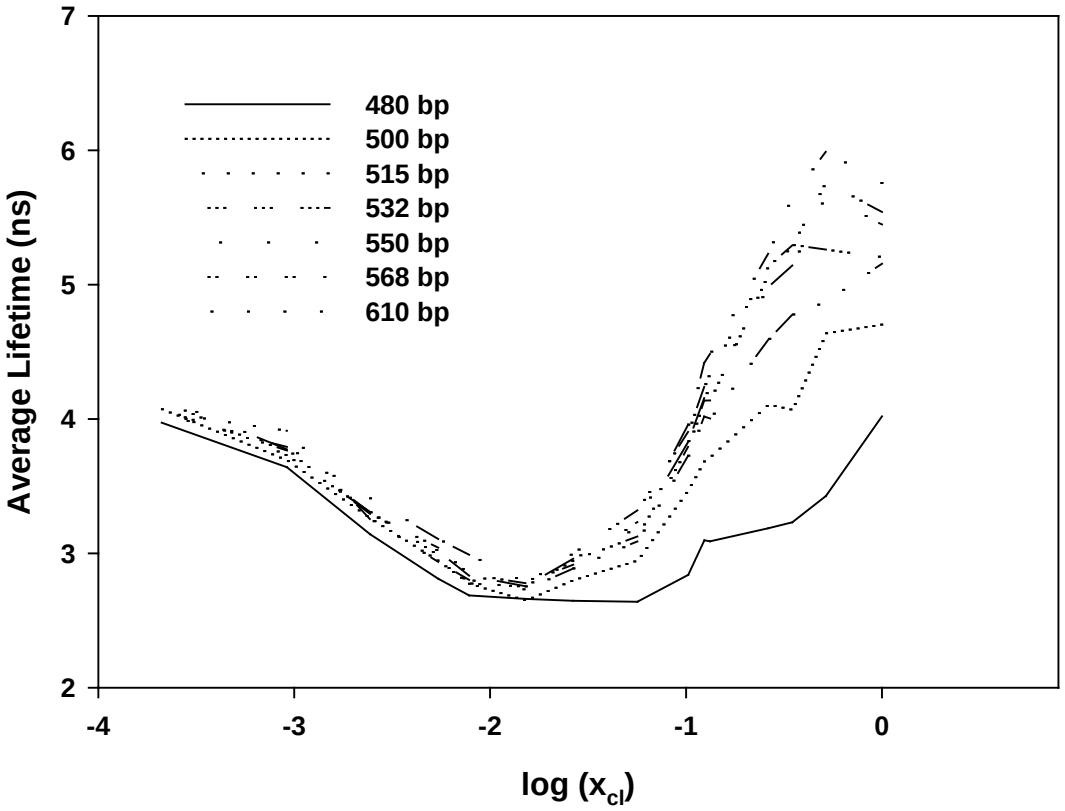


**Figure 9.** Average lifetime (ns) for C153 in PIL-Cl/MeOH mixed systems. The left side is MeOH-rich solutions and the right side is PIL-rich solutions.

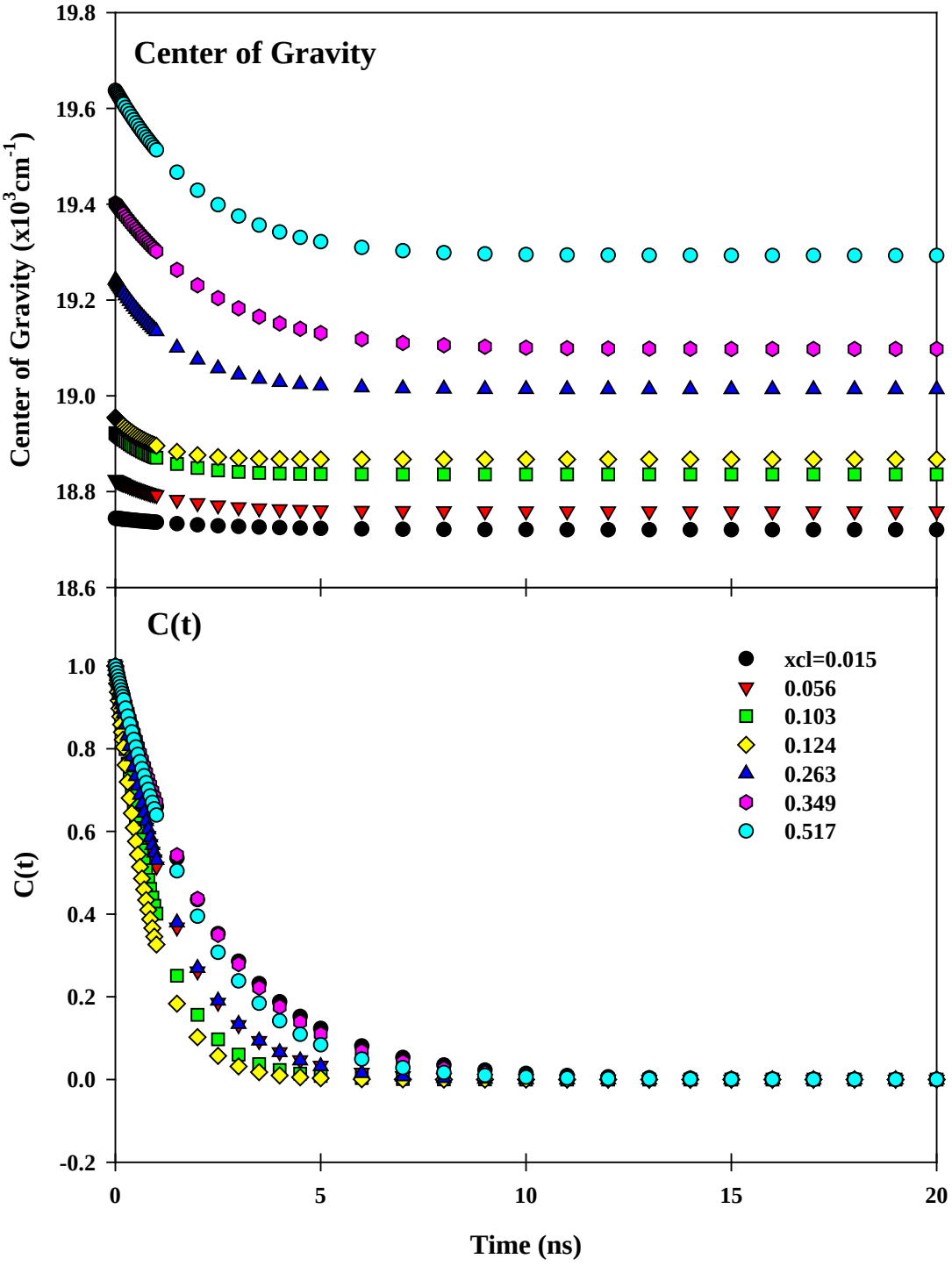


**Figure 10.** (a) The time-resolved emission center of gravity and (b) the solvation correlation function [C(t)] for representative MeOH/PIL mixtures.

# Chapter 4

## Conclusion

Steady state and time-resolved spectra shows solvation of C153 occurs at a faster rate in MeOH, than in neat RTPIL-Cl and MeOH/PIL solutions. The steady-state emission displays a 30 nm blue shift upon going from a neat MeOH solution to a neat PIL solution. At a mol fraction of around 0.03 PIL the solute emission is quenched by a factor of approximately 2. In addition, we observe a minimum value in the time-resolved intensity decay (lifetime) data at a mol fraction of 0.03 PIL-Cl consistent with the idea that C153 emission is most readily quenched at this solvent composition. Given that C153 is better solvated in MeOH-rich solution, as evidenced by the relatively red peak maximum in the steady-state data and by the fact that the lifetimes in MeOH-rich solution is very similar to neat MeOH we conclude that solvent reorganization is very fast as expected based solely on a viscosity argument. However, the relaxation kinetics are more complicated in PIL-Cl because the solvent structure itself is inherently more complex because of the various attractive forces in the PIL solution.

While these data provide a substantial amount of information about the solvation of C153 in MeOH/PIL mixed solvents there are some questions that remain unanswered. For example, exactly how much viscous drag can one expect to contribute to the observed reorganization? Is is solely a Stokes-Einstein relationship that determines the reorganization kinetics? How does changing the anion identity impact solvent reorganization? Clearly, more data, and a wider variety of data, is needed before we can conclusively state what the “exact” mechanism is that underlies solvent relaxation in this mixed system.

## References


[1] Ito, N.; Arzhantsev, S.; Heitz, M.; Maroncelli, M. *J. Phys. Chem. B* **2004**, *108*, 5771-5777.

[2] Arzhantsev, S.; Jin, H.; Baker, G. A.; Maroncelli, M. *J. Phys. Chem. B* **2007**, *111*, 4978-4989.

[3] Arzhantsev, S.; Jin, H.; Ito, N.; Maroncelli, M. *Chemical Physics Letters* **2006**, *417*, 524-529.

[4] Carvalho, P. J.; Álvarez, V. H.; Marrucho, I. M.; Aznar, M.; Coutinho, J. A. P. *J. of Supercritical Fluids* **2010**, *52*, 258-265.

[5] Kashyap, H. K.; Biswas, R. *J. Phys. Chem. B* **2008**, *112*, 12431-12438.

[6] Shekaari, H.; Mousavi, S. S. *Fluid Phase Equilibria* **2010**, *291*, 201-207.

[7] Kodama, D.; Kanakubo, M.; Kokubo, M.; Ono, T.; Kawanami, H.; Yokoyama, T.; Nanjo, H.; Kato, M. *J. of Supercritical Fluids* **2010**, *52*, 189-192.

[8] Pramanik, R.; Sarkar, S.; Ghatak, C.; Setua, P.; Rao, V. G.; Sarkar, N. *Chemical Physics Letters* **2010**, *490*, 154-158.

[9] Lee, S. U.; Jung, J.; Han, Y-K. *Chemical Physics Letters* **2005**, *406*, 332-340.

[10] Chowdhury, P. K.; Halder, M.; Sanders, L.; Calhoun, T.; Anderson, J. L.; Armstrong, D. W.; Song, X.; Petrich, J. W. *J. Phys. Chem. B* **2004**, *108*, 10245-10255.

[11] Jin, H.; O'Hare, B.; Dong, J.; Arzhantsev, S.; Baker, G. A.; Wishart, J. F.; Benesi, A. J.; Maroncelli, M. *J. Phys. Chem. B* **2008**, *112*, 81-92.

[12] Benavides-Garcia, M. G.; Monroe, M. *Chemical Physics Letters* **2009**, *479*, 238-243.

[13] Jin, H.; Baker, G. A.; Arzhantsev, S.; Dong, J.; Maroncelli, M. *J. Phys. Chem. B* **2007**, *111*, 7291-7302.

[14] Seki, S.; Kobayashi, T.; Kobayashi, Y.; Takei, K.; Miyashiro, H.; Hayamizu, K.; Mitsugi, S. T.; Umebayashi, Y. *J. of Molecular Liquids* **2010**, *152*, 9-13.

[15] Tran, C. D.; Lacerda, S. H. D. P.; Oliveira, D. *Applied Spectroscopy* **2003**, *57*, 152-157.

[16] Pramanik, R.; Sarkar, S.; Ghatak, C.; Setua, P.; Rao, V. G.; Sarkar, N. *Chemical Physics Letters* **2010**, *490*, 154-158.

[17] Chakrabarty, D.; Chakraborty, A.; Seth, D.; Hazra, P.; Sarkar, N. *Chemical Physics Letters* **2004**, *397*, 469-474.

[18] Arzhantsev, S.; Ito, N.; Heitz, M.; Maroncelli, M. *Chemical Physics Letters* **2003**, *381*, 278-286.

[19] Chakrabarty, D.; Hazra, P.; Chakraborty, A.; Seth, D.; Sarkar, N. *Chemical Physics Letters* **2003**, *381*, 697-704.

[20] McQuarrie, D. A.; Simon, J. D. *Physical Chemistry: A Molecular Approach*, University Science Books, **1997**, 592-595.

[21] Horng, M.-L.; Gardecki, J. A.; Maroncelli, M. *J. Phys. Chem. A* **1997**, *101*, 1030-1047.

[22] Lewis, J. E.; Maroncelli, M. *Chemical Physics Letters* **1998**, *282*, 197-203.

[23] Fee, R. S.; Maroncelli, M. *Chemical Physics* **1994**, *183*, 235-247.

[24] Nigam, S.; Rutan, S. *Focal point* **2001**, *55*, 362A-370A.

[25] Ladanyi, B. M.; Maroncelli, M. *J. of Chem. Physics* **1998**, *109*, 3204-3221.

[26] Mukherjee, P.; Crank, J. A.; Sharma, P. S.; Wijeratne, A. B.; Adhikary, R.; Bose, S.; Armstrong, D. W.; Petrich, J. W. *J. Phys. Chem. B* **2008**, *112*, 3390-3396.

[27] Reynolds, L.; Gardecki, J. A.; Frankland, S. J. V.; Horng, M. L.; Maroncelli, M. *J. Phys. Chem.* **1996**, *100*, 10337-10354.

[28] Jin, H.; Li, X.; Maroncelli, M. *J. Phys. Chem. B* **2007**, *111*, 13473-13478.

[29] Biswas, R.; Lewis, J. E.; Maroncelli, M. *Chemical Physics Letters* **1999**, *310*, 485-494.

[30] Maroncelli, M.; Kumar, V. P.; Papazyan, A. *J. Phys. Chem.* **1993**, *97*, 13-17.

[31] Ito, N.; Arzhantsev, S.; Maroncelli, M. *Chemical Physics Letters* **2004**, *396*, 83-91.

[32] Arzhantsev, S.; Jin, H.; Baker, G. A.; Ito, N.; Maroncelli, M. in *Femtochemistry VII, Fundamental Ultrafast Processes in Chemistry, Physics, and Biology*, A. W. Castleman, Jr. and Michele L. Kimble eds. (Elsevier B.V. Ltd., **2006**), p. 225-234.

[33] Bradaric, C. J.; Downard, A.; Kennedy, C.; Robertson, A. J.; Zhou, Y. *Green Chem.* **2003**, *5*, 143-152.

[34] Acros Chemicals.